MOLECULAR AND CELLULAR BIOLOGY, Mar. 2006, p. 2273–2285 Vol. 26, No. 6
0270-7306/06/$08.00+0 doi:10.1128/MCB.26.6.2273–2285.2006

CARM1 Regulates Proliferation of PC12 Cells by Methylating HuD

Tatsuji Fujiwara,[1,2] Yasutake Mori,[1]* Dong Ling Chu,[1] Yoshihisa Koyama,[1] Shingo Miyata,[1] Hiroyuki Tanaka,[1,2] Kohji Yachi,[1,2] Tateki Kubo,[3] Hideki Yoshikawa,[2] and Masaya Tohyama[1]

Department of Anatomy and Neuroscience,[1] Department of Orthopedic Surgery,[2] and Department of Plastic Surgery,[3] Graduate School of Medicine, Osaka University, Osaka 565-0871, Japan

Received 3 October 2005/Returned for modification 9 November 2005/Accepted 23 December 2005

HuD is an RNA-binding protein that has been shown to induce neuronal differentiation by stabilizing labile mRNAs carrying AU-rich instability elements. Here, we show a novel mechanism of arginine methylation of HuD by coactivator-associated arginine methyltransferase 1 (CARM1) that affected mRNA turnover of $p21^{cip1/waf1}$ mRNA in PC12 cells. CARM1 specifically methylated HuD in vitro and in vivo and colocalized with HuD in the cytoplasm. Inhibition of HuD methylation by CARM1 knockdown elongated the $p21^{cip1/waf1}$ mRNA half-life and resulted in a slow growth rate and robust neuritogenesis in response to nerve growth factor (NGF). Methylation-resistant HuD bound more $p21^{cip1/waf1}$ mRNA than did the wild type, and its overexpression upregulated $p21^{cip1/waf1}$ protein expression. These results suggested that CARM1-methylated HuD maintains PC12 cells in the proliferative state by committing $p21^{cip1/waf1}$ mRNA to its decay system. Since the methylated population of HuD was reduced in NGF-treated PC12 cells, downregulation of HuD methylation is a possible pathway through which NGF induces differentiation of PC12 cells.

Hu proteins have been identified as target antigens in the sera of patients with paraneoplastic encephalomyelitis, an autoimmune disease associated with small-cell lung cancer and neuroblastoma (20, 64). The four members of the Hu protein family have been identified as RNA-binding proteins (RBPs) that show homology to the *Drosophila melanogaster* ELAV protein (27, 28, 42, 52, 56). These mammalian Hu/ELAV proteins, with the exception of HuR, are expressed exclusively in neurons (20, 45, 52). Hu family proteins share the characteristic of three RNA recognition motif domains (RRMs), with a hinge region intervening between the second and the third RRMs (27, 28, 56). In previous reports, Hu proteins had been reported to bind to long poly(A)+ tails (1, 46), but recent studies demonstrated that they recognize AU-rich elements (AREs) which reside in the 3′-untranslated regions (3′-UTRs) of some labile mRNA species (33, 40, 42, 53, 54) and determine their stability or translational efficiency (6, 7, 23, 29, 37).

HuD, one of the Hu family proteins, has been shown to bind to AREs found in the 3′-UTRs of several mRNAs, including c-*fos* (14), tau (9), GAP43 (15), and $p21^{cip1/waf1}$ (30), and to the U-rich element found in the p27 mRNA 5′-UTR (36). Previously, it was reported that overexpression of HuD induces neuronal differentiation in PC12 cells, cortical primary culture neurons, and retinoic acid-induced teratocarcinoma cell lines (5). On the other hand, antisense-mediated knockdown of HuD resulted in the inhibition of neurite extension in PC12 cells (48) and HuD-deficient mice exhibited a larger population of dividing stem cells in the adult subventricular zone (3). These findings indicated that HuD is required for neuronal differentiation processes, including growth arrest and cell fate acquisition of neural stem/progenitor cells, and possibly for sprouting and regeneration of mature neurons.

Given that HuD-bound gene products are involved in cell cycle arrest ($p21^{cip1/waf1}$ and p27), neurite outgrowth (GAP43 and tau), and functional differentiation (choline acetyltransferase) (21), HuD is presumed to induce the neuronal cell shape by exerting a protective effect on these ARE-containing labile mRNAs by antagonizing ARE-mediated mRNA decay. In the case of nerve growth factor (NGF)-induced differentiation of PC12 cells, NGF alters the RNA binding property of HuD towards AREs in the course of differentiation. However, there is no evidence revealing how HuD-ARE interactions are regulated under the NGF signal transduction pathway. We note that HuR, a ubiquitously distributed Hu protein, was arginine methylated by coactivator-associated arginine methyltransferase 1 (CARM1) in the myeloid cell line when the cells were stimulated by lipopolysaccharide (41). However, functional differences between methylated and unmethylated HuR have not yet been elucidated. Since the four mammalian Hu proteins (HuR, HuB, HuC, and HuD) are quite akin to each other in amino acid sequence (27, 52), we explored the possibility that HuD is also methylated at the corresponding arginine residue to HuR.

RBPs are the major substrate group for protein arginine methyltransferases (PRMTs) (8, 26, 34, 37, 43, 47, 49, 50, 57, 60, 61, 67). Most RBPs contain GAR domains, which consist of a repetition of RGG or RXR (X is an aliphatic residue) (11, 58) and are the canonical targets for type I PRMTs that catalyze the formation of asymmetric NG,NG-dimethylarginine residues (37, 49). Type I enzymes PRMT1 and PRMT3 favor GAR domains as their substrates (18, 25, 66), and especially PRMT1 has a promiscuity to methylate arginine residues encompassed by GAR domains (65, 66). On the other hand, another type I enzyme, CARM1, methylates a narrow spectrum of proteins, histone H3 (12, 44), p300/CBP (69), PABP1, and TARPP (39), all of which lack GAR-like domains around the arginine residues. HuR also lacks the canonical GAR domain but instead has an alanine residue 2 residues N-terminal

* Corresponding author. Mailing address: Department of Anatomy and Neuroscience, Graduate School of Medicine, Osaka University, 2-2 Yamadaoka, Suita, Osaka 565-0871, Japan. Phone: 81-6-6879-3221. Fax: 81-6-6879-3229. E-mail: mori@anat2.med.osaka-u.ac.jp.

before the methylated arginine, which is common to most of the CARM1 substrates (41).

In this report, we first demonstrated that HuD is also an in vivo and in vitro substrate for CARM1 by ^{3}H labeling and immunodetection of the methylarginine residue of which Arg^{236} is mapped as the methylated residue by CARM1. Though CARM1 was so far reported to reside predominantly in the cell nuclei, in PC12 cells CARM1 distribution ranges from the nuclei to the cytoplasm, including the cell peripheries, and CARM1 is colocalized with HuD in the cytoplasm. To examine the biological significance of HuD methylation by CARM1, we established CARM1-depleted PC12 cell lines and investigated the effect of CARM1 loss on HuD-regulated gene expression. In a series of CARM1-depleted cell lines, methylated HuD was completely lost, with the total HuD level being unchanged, and the $p21^{cip1/waf1}$ protein levels was remarkably increased compared with levels in parental PC12 cells. Further, we demonstrated that unmethylated HuD bound more $p21^{cip1/waf1}$ mRNA than did methylated HuD and led to prolongation of $p21^{cip1/waf1}$ mRNA half-life. This phenomenon was reproduced in the PC12 cells overexpressing R236K methylation-resistant HuD. $p21^{cip1/waf1}$ cyclin-dependent kinase inhibitor has been shown to inhibit the proliferation of PC12 cells and accelerate neurite outgrowth in response to NGF (22, 71, 72). As anticipated, these cells exhibited a slower growth rate in the growth medium and accelerated neuritogenesis in response to NGF than did the parental and mock-transfected PC12 cells. These findings indicated that CARM1 negatively regulates neuronal differentiation of PC12 cells by methylating HuD to prevent $p21^{cip1/waf1}$ mRNA from entering into the decay pathway. The overlapped distribution of CARM1 with BrdU-positive cells in the subventricular zone of the adult mouse generalizes the inhibitory role of CARM1 for the differentiation of neural progenitor/precursor cells as well as PC12 cells.

MATERIALS AND METHODS

Chemicals and antibodies. We used the following antibodies: anti-PRMT1 monoclonal antibody (MAb) (Abcam Ltd., Cambridge, United Kingdom), anti-CARM1 polyclonal antibody (PAb) (Upstate Biotech, Charlottesville, VA), anti-PRMT3 MAb (Upstate Biotech), anti-tau MAb (Upstate Biotech), anti-PRMT1 MAb (Abcam Ltd.), anti-mono- and dimethylarginine (anti-M/DMA) MAb (Abcam Ltd.), anti-$p21^{cip1/waf1}$ MAb (Santa Cruz Biotech, Inc., Santa Cruz, CA), anti-GAP43 PAb (Santa Cruz Biotech), rabbit anti-HuD PAb (Santa Cruz Biotech), goat anti-HuD PAb (Santa Cruz Biotech), anti-β-tubulin PAb (Santa Cruz Biotech), antihemagglutinin (HA) MAb (Sigma-Aldrich, St. Louis, MO), anti-actin MAb (C4; Chemicon Interntional Inc., Temecula, CA), Alexa Fluor 488-conjugated anti-mouse/rabbit immunoglobulin G (IgG) antibody (Molecular Probes Inc., Eugene, OR), and horseradish peroxidase (HRP)-conjugated anti-mouse/rabbit IgG antibody (Cell Signaling Tech., Beverly, MA). Recombinant histone H3 and H4 proteins were purchased from Upstate Biotech. The reagents used in this work were NGF (Upstate Biotech) and actinomycin D (Sigma-Aldrich).

Cell culture. PC12 cells were grown in Dulbecco's modified Eagle's medium supplemented with 10% horse serum, 5% fetal calf serum, 100 U/ml penicillin, and 100 μg/ml streptomycin. Cells were cultured in a humidified incubator at 37°C with a 5% CO_2 atmosphere. Differentiation was induced by incubating the cells with 100 ng/ml NGF in Dulbecco's modified Eagle's medium supplemented with 1% horse serum.

Plasmid construction. An N-terminal, HA-tagged HuD sequence was amplified with *Pfu* DNA polymerase (Promega Corp., Madison, WI) by using the primer set 5′-GGATCCGCGTCCACCATGTACCCATACGACGTACCAGATTACGCT GAGCCACAGGTGTCAAATGGA-3′ (forward) and 5′-CTCGAGCGGTCA GGACCTGTGGGCTTTGT-3′ (reverse), subcloned into pGEM-T vector (Promega Corp.), and sequenced from T7 and SP6 promoters with an ABI PRISM genetic analyzer (Applied Biosystems, Foster City, CA). The subcloned fragment was cloned into pcDNA3.1 vector (Invitrogen, Carlsbad, CA) with BamHI and XhoI sites (pC-HuDwt). Arginine-to-lysine mutants of HuD were induced by PCR using a common forward primer, 5′-TTGCTTAATATGGCCTATGGC-3′, and reverse primer 5′-ATTGTCCAGCCTGAAtttTTGAGCCTG-3′ for R236K or 5′-ATT GTCCAGcttGAATCTTTGAGC-3′ for R238K (the mutated codons are indicated in lowercase). PCRs were performed circumferentially toward pC-HuDwt and cloned into a pCDNA3.1 vector (pC-R236K and pC-R238K).

For the CARM1 knockdown, 23 bp of small hairpin RNA (shRNA) was expressed from pSILENCER 1.0-U6 (Ambion Inc., Austin, TX). pSILENCER-shCARM1 plasmid was generated by insertion of the sense and antisense stem sequence in the reverse direction, with an intervening loop sequence with ApaI and EcoRI multiple cloning sites. The insert was made by annealing two primers, 5′-GATGTGTGTGTGTTCAAGTTCAAGAGACTTGAACACACACACATC TTTTTT-3′ and 5′-AATTAAAAAAGATGTGTGTGTGTTCAAGTCTCT TGAACTTGAACACACACACATCGGCC-3′. The underlined sequences form a stem region of CARM1 shRNA which corresponds to 229 to 247 nucleotides of rat CARM1. This sequence is shared by all of the reported splicing variants of rat CARM1 (51). To generate stable cell lines, neomycin-resistant gene cassettes should be added to pSILENCER-shCARM1 by recloning BamHI-XbaI digested fragments containing the U6 promoter and CARM1 shRNA sequence into pcDNA3.1 vector with BglII and XbaI sites (pSILENCER-shCARM1 Neo^r).

PRMT1 and CARM1 were cloned using a PCR-based method for the prokaryotic expression system. CARM1, whose initiator codon is crammed with GC-rich clusters, was amplified with *Taq*PCRx polymerase (Invitrogen) by using the forward primer 5′-CCTGGAGCCGGATCTAAGATGGCAGC-3′, the other forward primer 5′-CCTGGAGCCGGATCTAGATCTGCAG-3′ for nested PCR, and a reverse primer, 5′-AGATCTGCTCCCGTAGTGCATGGTGTTGGTC-3′. PRMT1 was amplified with recombinant *Taq* DNA polymerase (Takara Bio Inc., Ohtsu, Japan) by using primer set 5′-GGATCCGCGGCAGCCGAGGCCGCGAAC-3′ and 5′-GGATCCGCGCATCCGGTAGTCGGTG-3′. The template was a HeLa cell 5′-enriched cDNA library (Clontech, Mountain View, CA). The amplified fragments were TA cloned into the pGEM-T vector (Promega Corp.) and sequenced from either the T7 or the SP6 promoter. BamHI-excised and BglII-excised PRMT1 were ligated into pCold II vector (Takara Bio Inc.) with a BamHI site (pCold-PRMT1 and pCold-CARM1).

To purify recombinant HuD proteins, PCR was performed using primer set 5′-GGATCCCCTATACTAGGTTATTGG-3′ and 5′-GGATCCGGACTTGTG GGCTTTGTTGGTTTTAAAG-3′ toward pC-HuDwt, pC-R236K, and pC-R238K. Each amplified product was cloned into pGEM-T vector (Promega Corp.), sequenced from either the T7 or the SP6 promoter, and cloned into pGEX4T-1 (Amersham Bioscience Corp., Piscataway, NJ) with BamHI sites.

Generation of stable cell lines. For CARM1 RNA interference analysis, pSILENCER-shCARM1 Neo^r plasmid and insertless plasmid were transfected using Lipofectamine 2000 reagent (Invitrogen) according to the manufacturer's instructions. The transfected cells were cultured in medium containing 500 μg/ml G418 (Invitrogen) for at least 14 days, and individual G418-resistant clones were yielded by the serial-dilution method. To confirm the downregulation of CARM1, whole-cell extracts of these clones were subjected to Western blot analysis with anti-CARM1 antibody. The CARM1 depletion was further confirmed by immunocytochemistry as described below. Two clones (no. 15 and 33) expressing significantly reduced levels of CARM1 were used for further studies.

In vivo BrdU treatment. Mice were injected intraperitoneally with BrdU in phosphate-buffered saline (PBS) (50 μg/g of body weight), and 2 h later they were deeply anesthetized.

Immunocytochemistry. PC12 cells were fixed in 4% formaldehyde, permeabilized, and blocked in 0.02 M PBS containing 0.3% Triton X-100 and 5% bovine serum albumin (BSA) for 30 min at room temperature (RT). They were incubated overnight at 4°C with anti-CARM1 antibody (1:100) and anti-HuD antibody (1:100). For fluorescence immunocytochemistry, the preparations were incubated for 1 h with Alexa Fluor 488-labeled goat anti-rabbit IgG antibody (Molecular Probes Inc.). Tetramethyl rhodamine isothiocyanate-labeled phalloidin (1:1,000; Sigma-Aldrich) was used to detect F-actin in PC12 cells. When necessary, DAPI (4′,6′-diamidino-2-phenylindole) (Wako Pure Chemical Industries, Osaka, Japan) was used to stain the nuclei. Samples were examined under a confocal laser-scanning microscope (Zeiss Axioplan2 LSM510). Enzyme immunodetection was conducted with a Vectastain Elite ABC kit (Vector Laboratories, Inc., Burlingame, CA) by following the manufacturer's instructions. Anti-CARM1 antiserum was adsorbed with 125 μg of the excess amount of recombinant His_6-CARM1 to perform the immunodepletion assay.

Immunohistochemistry. For immunohistochemistry, ICR mice were deeply anesthetized with 40 mg of sodium pentobarbital/kg of body weight, perfused with 4% paraformaldehyde. The brains were postfixed overnight in the same

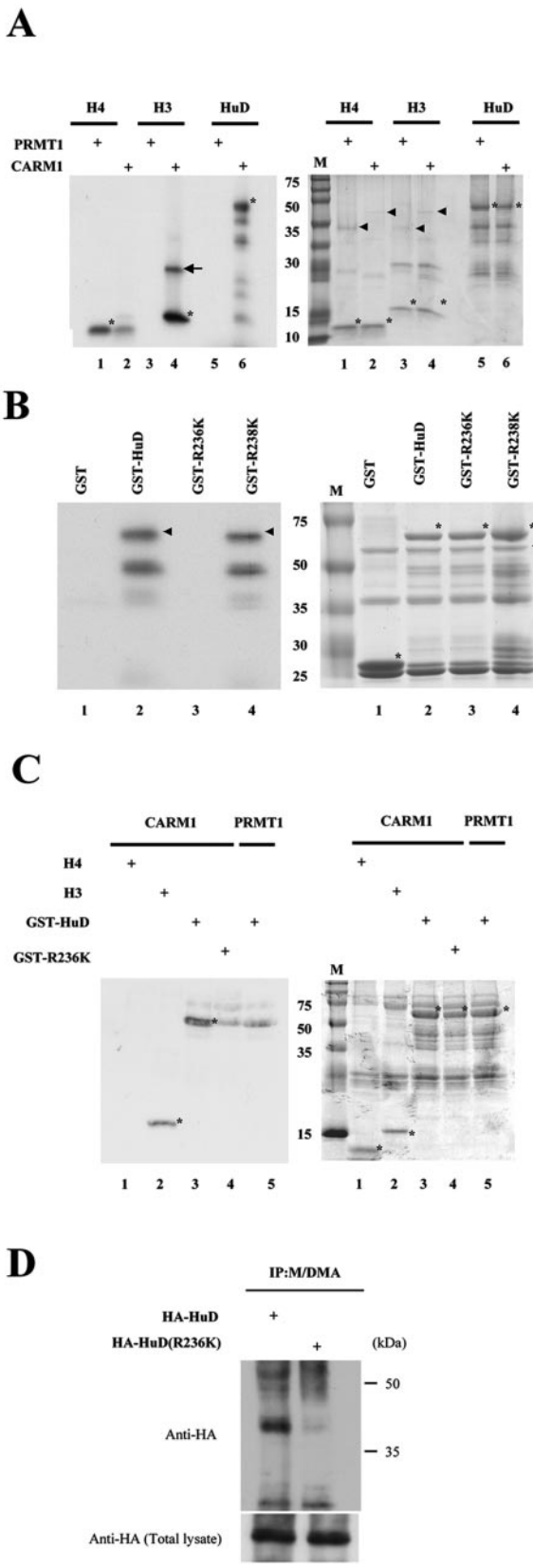

FIG. 1. CARM1-methylated Arg^{236} of HuD in vitro. (A) Recombinant histones H3 and H4 and GST-tagged HuDwt were methylated by either His_6-PRMT1 or His_6-CARM1. GST-HuD, histone H3, or histone H4 (3 μg each) was incubated with 1 μg of His-PRMTs in the presence of 1μCi of [^{3}H]AdoMet. As reported, histone H4 was methylated chiefly by His_6-PRMT1 (left panel, lanes 1 and 2) and histone H3 predominantly by His_6-CARM1 (left panel, lanes 3 and 4). GST-HuDwt was a specific substrate for His_6-CARM1, not His_6-PRMT1 (left panel, lanes 5 and 6). The methylated band indicated by an arrow was a histone H3 dimer. The right panel shows Coomassie staining of the gel identical to that shown in the left panel. Each of the substrates (asterisks) and enzymes (arrowheads) are indicated. Lane M is a molecular size marker (in kilodaltons). (B) In vitro methylation assay of GST-HuD mutants. GST-HuD, -R236K, -R238K, and GST alone were incubated with CARM1. ^{3}H-labeled bands were found in GST-HuDwt and GST-R238K to similar extents (left panel, lanes 2 and 4, arrowheads), while GST-R236K harboring a mutation at R^{236} (corresponding to R^{217} of HuR) was not ^{3}H labeled by CARM1 (left panel, lane 3). The faster-migrating bands are presumed to be degradative products of the HuD portion. GST alone also failed to undergo methylation (left panel, lane 1). Input of the recombinant proteins was verified by Coomassie staining of the gel shown in the left panel (right panel). GST and GST-tagged proteins are indicated by asterisks and CARM1 by the arrow. (C) CARM1-methylated GST-HuD was blotted with anti-M/DMA. GST-HuD and GST-R236K were incubated with recombinant CARM1 (left panel, lanes 3 and 4) and PRMT1 (left panel, lane 5). Input of GST-HuD proteins was verified by Coomassie staining (right panel). (D) HuD harboring the R236K mutation was methylation defective. Cell extracts from HA-HuD- and HA-R236K-expressing PC12 cells were immunoprecipitated with anti-HA antibody, and the precipitated proteins were analyzed by immunoblotting with anti-M/DMA antibody (upper panel) or anti-HA antibody (lower panel). Only HA-HuD was detectable with anti-HA antibody, while HA-R236K was not, as expected.

fixative and cryoprotected in a 30% (wt/vol) sucrose solution overnight. The tissues were then embedded in Tissue-Tek OCT compound (Ted Pella Inc., Redding, CA) and frozen on dry ice at −80°C. The frozen sections with 14-μm thickness were mounted on aminopropylsilane-coated Superfrost-Plus slides (Matsunami, Osaka, Japan). The brain sections were rinsed three times in 0.02 M PBS for 30 min at RT, followed by blocking in 0.02 M PBS containing 0.3% Triton X-100 and 5% BSA. The sections were incubated overnight at 4°C with polyclonal rabbit anti-CARM1 antibody (1:100) and monoclonal anti-BrdU antibody (1:100) containing 0.3% Triton X-100 and 3% BSA. Slides were then treated with fluorescent dye Alexa Fluor 488-conjugated goat anti-mouse IgG (CARM1) or fluorescent dye Alexa Fluor 568-conjugated goat anti-rabbit IgG (BrdU) for 1 h at RT in 0.02 M PBS containing 3% BSA. Nonspecific binding was examined by omitting the primary antibody during the incubation process. Sections were analyzed using a Zeiss LSM510 microscope.

RNA isolation and Northern blot analysis. Total RNA from either parental PC12 cells or CARM1 knockdown cells was extracted by the acid guanidinium isothiocyanate-phenol chloroform method. A total of 10 μg of RNA was separated by electrophoresis on 1.0% agarose-formamide gels and transferred overnight onto a polyvinylidene difluoride membrane (Millipore, Bedford, MA). The membrane was prehybridized for 1 h at 65°C in hybridization buffer (0.9 M NaCl, 90 mM sodium citrate, pH 7.0) containing 5× Denhardt's solution, 0.5% sodium dodecyl sulfate (SDS), and 100 ng/ml heat-denatured salmon sperm DNA (Sigma-Aldrich). The template DNAs specific for rat $p21^{cip1/waf1}$ mRNA, GAP43 mRNA, tau mRNA, or GAPDH (glyceraldehyde-3-phosphate dehydrogenase) mRNA were amplified by PCR using the following primer sets: 5′-GCTAGCG CCACCATGTCCGATCCTGGTGAT-3′ and 5′-GATATCGGGCTTTCTCTT GCAGAAGACCAA-3′ ($p21^{cip1/waf1}$); 5′-AAGCTTGCCACCATGCTGTGCTG TATGAGAAGAACC-3′ and 5′-GGATCCGGCATGTTCTTGGTCAGCCT C-3′ (GAP43); 5′-AGACCACACCCAGCCCAAAGACTCC-3′ and 5′-GGC CAAAGAGGCGGACACTTCATC-3′ (tau); and 5′-TTCAACGGCACAGTC AAGG-3′ and 5′-CATGGACTGTGGTCATGAG-3′ (GAPDH). Radiolabeled cDNA with [^{32}P]dCTP (Amersham Bioscience Corp.) was made from each of the amplified products with a random labeling kit (Takara Bio Inc.) by following the manufacturer's instructions. After hybridization overnight at 65°C, the membrane was sequentially washed with 2× SSC (1× SSC is 0.15 M NaCl plus 0.015 M sodium citrate) containing 0.5% SDS and 0.2× SSC containing 0.5% SDS, twice in each wash buffer for 30 min at 65°C. Then the filters were exposed to X-OMAT films (Eastman Kodak, Rochester, NY) and subjected to autoradiography.

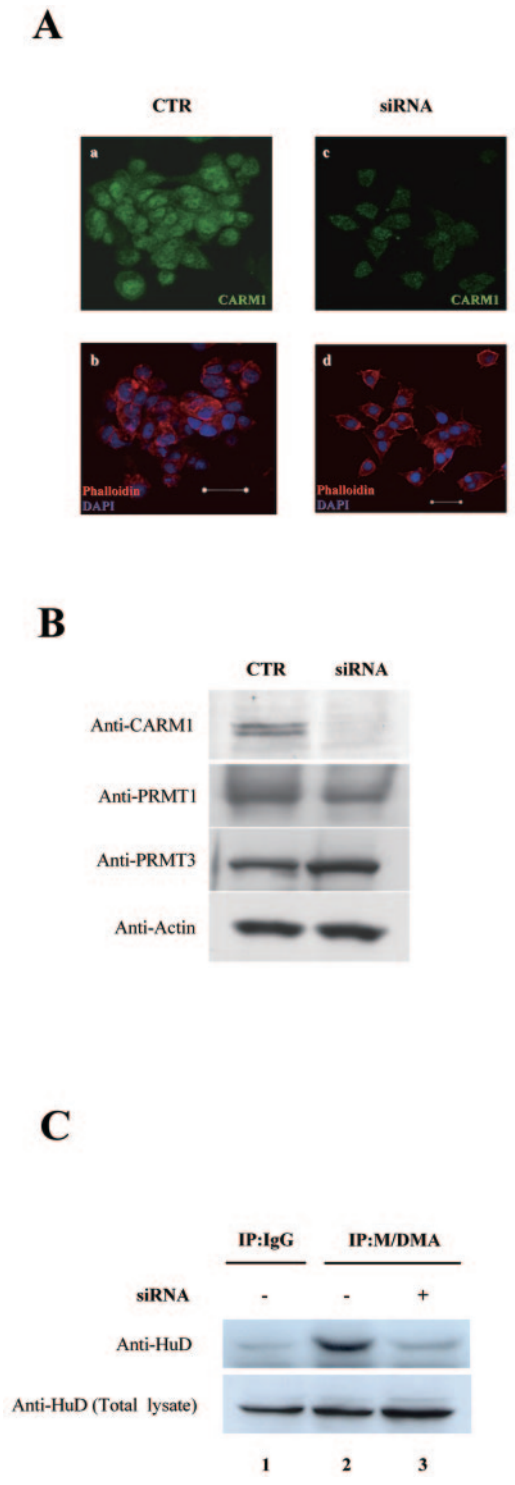

FIG. 2. Arg[236] of HuD was methylated by CARM1 in PC12 cells. (A) CARM1 expression was abrogated by stably expressing CARM1 shRNA in PC12 cells, as shown by immunocytochemistry using antiserum against CARM1 (green), phalloidin-actin (red), and DAPI (blue). The empty vector-transfected cells did show a dense signal in the nuclei and were moderately stained in the cytoplasm (a), while shRNA specific for CARM1 sequence significantly suppressed the nuclear staining (c). (B) Specific reduction of CARM1 level in one of the clones stably expressing CARM1 shRNA, as shown by immunoblot analysis. Total proteins isolated from the CARM1 shRNA-expressing PC12 cells and the parental cells were blotted with antibodies against CARM1, PRMT1, PRMT3, and actin. CARM1 shRNA did not affect PRMT1 and PRMT3 protein levels (right column). (C) Endogenous HuD was arginine methylated in the native PC12 cells but not in the CARM1$^-$ cells. Whole-cell extracts from parental and CARM1$^-$ PC12 cells were loaded directly (lower panel) or immunoprecipitated with either anti-M/DMA antibody or control IgG (upper panel). These samples were analyzed by immunoblotting with anti-HuD antibody. Anti-M/DMA antibody precipitated endogenous HuD from mock-transfected PC12 cell lysate (lane 2) but not from the lysate of CARM1$^-$ cell line 15 (lane 3). The fraction precipitated with control IgG1 contained no HuD immunoreactivity (lane 1). CTR, control empty vector-expressing cells; siRNA, CARM1 shRNA-expressing cells.

Analysis of mRNA stability. For the mRNA half-life assay, actinomycin D (Sigma-Aldrich) was added to media at 3 μg/ml of the final concentration, which was designated as 0 h. Total RNA was extracted by Isogen reagent (Nippon Gene Co., Ltd., Tokyo, Japan) at each time point and used for Northern blot analysis. The signal of p21$^{cip1/waf1}$ mRNA at each time point was then evaluated by a densitometric program and normalized to that of GAPDH mRNA. The values were plotted on a logarithmic scale, and the time period required for the densitometric values to undergo a reduction to one-half of the initial abundance was calculated.

Nuclear run-on assay. Assays were performed as described previously (21), with minor modifications. Briefly, 5 μg of PCR-amplified DNAs corresponding to the indicated genes (enhanced green fluorescent protein, p21$^{cip1/waf1}$, GAP43, and GAPDH) was denatured and blotted onto a polyvinylidene difluoride membrane (Millipore, Bedford, MA). Nuclei prepared from 2×10^7 PC12 cells were isolated from each treatment group by using lysis buffer (10 mM Tris-HCl, 1 mM EDTA, 150 mM NaCl, 0.5% NP-40, pH 7.4), and nascent mRNAs were labeled in in vitro transcription buffer (100 mM KCl, 2.5 M $MgCl_2$, 2.5 mM rATP, 2.5 mM rCTP, 2.5 mM rGTP) containing 500 μCi [α-^{32}P]UTP (Amersham Bioscience Corp.) for 30 min at 30°C. Radiolabeled RNA was then isolated using Isogen reagent (Nippon Gene Co., Ltd.) and hybridized onto the blotted membrane as shown for the Northern blot analysis.

IP followed by RT-PCR. Fifty-percent-confluent PC12 cells plated on a 15-cm-diameter plastic dish were transiently transfected with 15 μg of pC-HuDwt and pC-R236K by using Lipofectamine 2000 (Invitrogen). At 24 h after transfection, the cells were incubated for 48 h with or without NGF and lysed by immunoprecipitation (IP) buffer (10 mM Tris-HCl, 1 mM EDTA, 100 mM NaCl, 1.5 mM $MgCl_2$, 250 mM KCl, 2 mM DTT dithiothreitol [DTT], 0.5% Triton X-100, and 1,000 U/ml RNase inhibitor, plus protease inhibitor tablet, pH 7.4). HA-tagged proteins were immunopurified by incubation for 2 h at 4°C with protein G Sepharose beads (Amersham Bioscience Corp.) that had been precoated with 20 μg of either mouse IgG or anti-HA. The immunoprecipitates were washed five times with NT2 buffer (50 mM Tris-HCl, 1 mM EDTA, 150 mM NaCl, 1 mM $MgCl_2$, and 0.05% NP-40, pH 7.4). The RNAs in the precipitates were extracted using the Isogen reagent and reverse transcribed by Ready-To-Go (Amersham Bioscience Corp.). The presence of either p21$^{cip1/waf1}$ or GAPDH mRNA in the IP materials was assayed by reverse transcriptase PCR (RT-PCR) using sequence-specific primer pairs 5′-GCTAGCGCCACCATGTCCGATCTG GTGAT-3′ and 5′-GATATCGGGCTTTCTCTTGCAGAAGACCAA-3′ for p21$^{cip1/waf1}$ and 5′-TTCAACGGCACAGTCAAGG-3′ and 5′-CATGGACTG TTGTCATGAG-3′ for GAPDH.

Recombinant protein. *Escherichia coli* BL21 cells (Novagen, Madison, WI) were transformed by pCold-PRMT1, while JM110 *dam* methylase-deficient cells (Toyobo, Osaka, Japan) were transformed by the pCold-CARM1 vector. The transformed cells were propagated at 37°C up to an optical density at 280 nm of 0.5, followed by an incubation of 15 h with vigorous agitation in the presence of 1 mM IPTG (isopropyl-β-D-thiogalactopyranoside). The collected cells were lysed in lysis buffer (50 mM Tris-HCl, 250 mM NaCl, 10 mM guanidine containing 10 mg/ml lysozyme, pH 8.0), sonicated on ice, and centrifuged at 12,000 × *g* for 20 min. The supernatants were incubated with Ni-nitrilotriacetic acid His-Bind resin (Novagen) for 6 h at 4°C. The gels were washed four times in wash buffer (50 mM Tris-HCl, 250 mM NaCl, 20 mM guanidine, pH 8.0) and eluted by elution buffer (50 mM Tris-HCl, 250 mM NaCl, 100 mM guanidine, pH 8.0). The BL21 strains transformed with pGEX-HuDwt, R236K, and R238K were cultured on a large scale at 37°C in the presence of 1 mM IPTG. The collected cells were sonicated in ice-cold lysis buffer (50 mM Tris-HCl, 150 mM NaCl, 5 mM $MgCl_2$, 1 mM DTT, 1 mM EDTA, 1% Triton X-100, plus protease inhibitor cocktail, pH 7.5), and centrifuged at 12,000 × *g* for 20 min. The supernatants

were incubated with glutathione Sepharose (Amersham Bioscience Corp.) for 6 h, washed four times with PBS containing 0.5% Triton X-100, and eluted by 20 mM reduced glutathione (Nacalai Tesque, Kyoto, Japan) in 50 mM Tris-HCl (pH 8.0).

In vitro protein methylation assay. In vitro methylation of recombinant wild-type HuD and mutated forms (R236K and R238K) tagged with glutathione *S*-transferase (GST) was performed as follows. A total of 3 μg of each substrate (H3 histone, H4 histone, GST-tagged wild-type HuD [GST-HuDwt], GST-R236K, and GST-R238K) was incubated with 1 μg of His_6-tagged PRMT1 or CARM1 in reaction buffer (50 mM Tris-HCl, 1 mM DTT, pH 7.4) in the presence of 1 μCi of [^{3}H]adenosylmethionine (AdoMet) (Amersham Bioscience Corp.) for 1 h at 37°C. For the cold assay, the reactions were performed in reaction buffer containing 10 mM AdoMet (Sigma-Aldrich).

RESULTS

HuD undergoes in vitro and in vivo arginine methylation by CARM1. There is a poor understanding of the mechanism by which HuD is regulated to antagonize ARE-mediated mRNA decay. Li et al. reported that HuR, one of the Hu family proteins, is methylated specifically by CARM1 in vitro and in vivo (41). The methylated arginine residue of HuR and the surrounding amino acid sequence are conserved among all other Hu proteins (28, 52). Accordingly, we examined whether HuD might also be methylated by CARM1 at its homologous arginine residue. GST-HuDwt was incubated with recombinant His_6-tagged PRMT1 and CARM1 in the presence of [^{3}H]AdoMet. ^{3}H incorporation was observed with GST-HuDwt incubated with CARM1 (Fig. 1A, lane 6) but not with PRMT1, which is predominantly responsible for the type I arginine methylation in mammalian cells (Fig. 1A, lane 5) (65). To confirm the activities of the prepared His_6-tagged CARM1 and PRMT1, we incubated them with their respective known substrates, histones H4 and H3 (4, 44, 62). Both of the recombinant enzymes were competent to incorporate ^{3}H into their specific substrates (Fig. 1A, lanes 1 to 4). The ^{3}H-labeled, slower-migrating band of the histone H3 lane on the fluorographic image was presumably its previously reported dimerized product (Fig. 1A, lane 4) (41). To map the CARM1-methylated arginine residue on HuD, we performed mutational analysis of recombinant HuD. Since Arg^{236} of HuDwt corresponds to arginine-methylated Arg^{217} of HuR (41), we replaced either Arg^{236} or Arg^{238} of GST-HuD with a lysine residue (R236K and R238K). As anticipated, the Arg^{236} mutation exhibited methylation resistance to CARM1 activity against HuDwt (Fig. 1B, lane 3), whereas the Arg^{238} mutation was methylated to a level comparable to that for HuDwt (Fig. 1B, lane 4). It is important to note that the HuD (R236K) mutant still contains many other arginine residues. GST alone did not undergo any modification by CARM1 (Fig. 1B, lane 1), demonstrating that CARM1 action was targeted to the HuD portion of the fusion recombinant protein. Therefore, only the Arg^{236} residue serves as a target for CARM1-mediated arginine methylation.

To further examine whether the ^{3}H-labeled proteins are derived from arginine dimethylation by CARM1, we performed Western blot analysis on the in vitro methylated products. Anti-M/DMA antibody recognized GST-HuDwt incubated with CARM1 (Fig. 1C, lane 3), but faint immunoreactivity was observed with CARM1-incubated GST-R236K (Fig. 1C, lane 4). This was comparable to results with GST-HuDwt incubated with PRMT1 (Fig. 1C, lane 5), which is presumed to be a nonspecific signal. Anti-

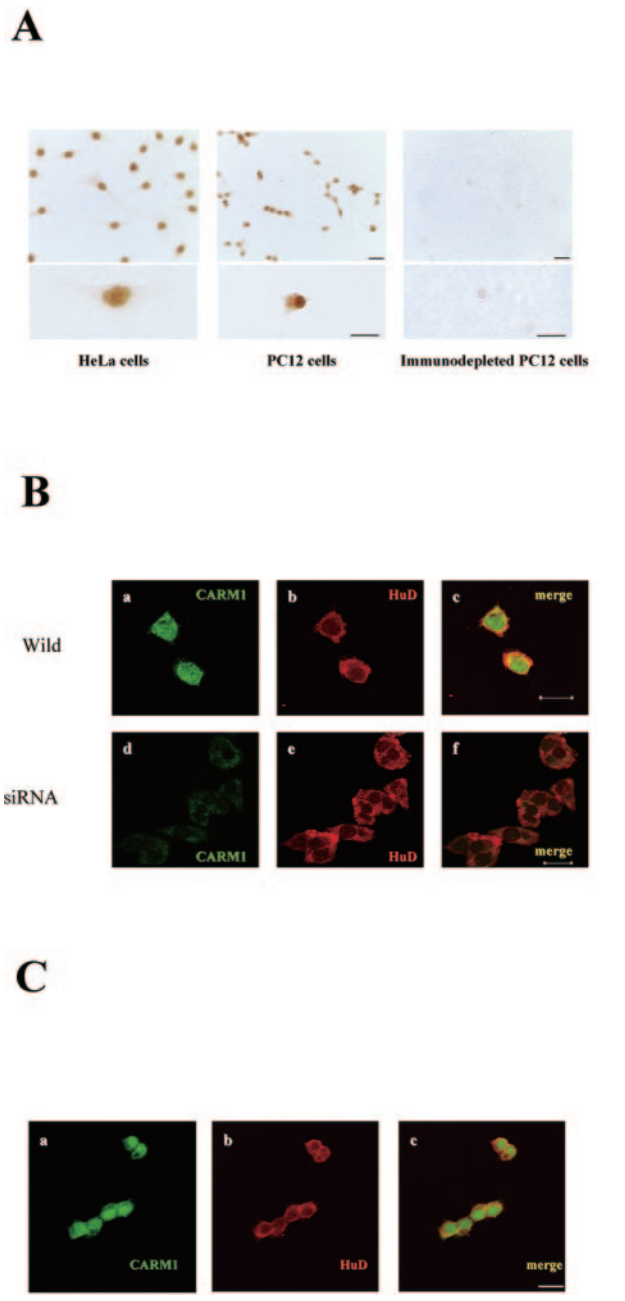

FIG. 3. Subcellular localization of CARM1 in PC12 cells. (A) Subcellular localization of CARM1 in PC12 cells was confirmed by HRP-DAB detection. In HeLa cells, CARM1 immunoreactivities were found to occur exclusively in the nuclei, but CARM1 exhibited cytoplasmic localization, as well as intense nuclear localization, in PC12 cells. When antiserum adsorbed with recombinant CARM1 was applied to the PC12 cells, both cytoplasmic and nuclear immunoreactivities were lost. The lower panels show high-power views of the cells shown in the upper panels. (B) Fluorescence immunocytochemistry using anti-CARM1 (a and d) (green) and anti-HuD (b and e) (red) antibodies with mock-transfected PC12 cells (a and b) and CARM1$^-$ cells (d and e). Cytoplasmic colocalization of both immunoreactivities (yellow) was found with the mock-transfected cells (c), whereas no remarkable colocalization was found with the CARM1$^-$ cells (f). The colocalization represented the perinuclear pattern and declined at the cell peripheries. Some cells had colocalizing spots in the growing neurites (data not shown). siRNA, CARM1 shRNA-expressing cells. (C) Immunocytochemistry using goat anti-HuD antibody. The same distribution pattern as described for panel B was observed.

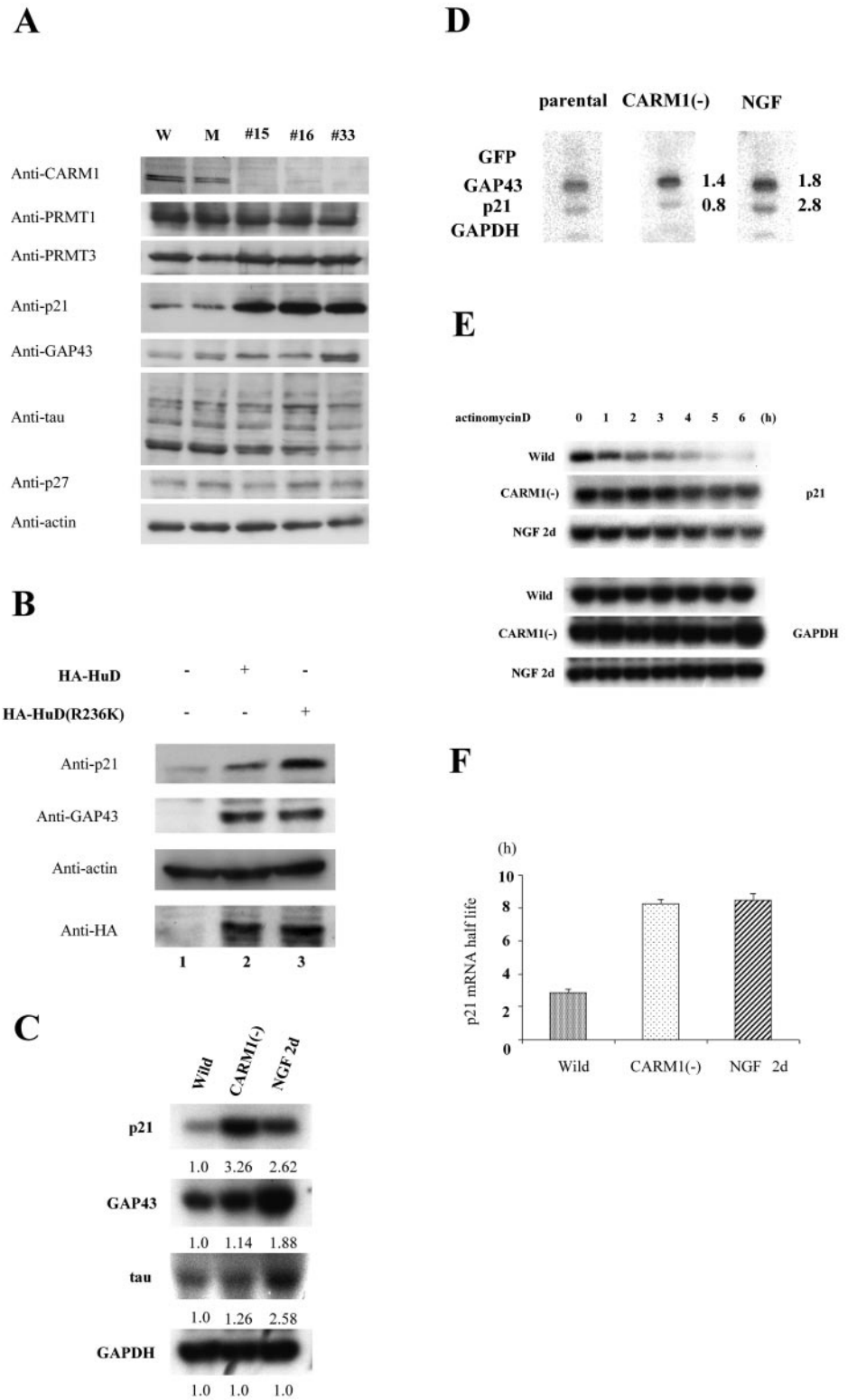

FIG. 4. CARM1 depletion in PC12 cells exclusively induces $p21^{cip1/waf1}$ expression. (A) Protein expression patterns of HuD-regulating genes in the wild-type (W), mock-transfected (M), and $CARM1^{-}$ PC12 cells, which were all cultured under the same growth condition. The whole-cell lysates of these cells were blotted with anti-CARM1, -PRMT1, -PRMT3, -$p21^{cip1/waf1}$, -GAP43, -tau, -p27, and -actin antibodies. Note that $p21^{cip1/waf1}$ protein levels significantly increased in $CARM1^{-}$ clones 15, 16, and 33. These cell lines also represented a slight increment of basal protein level of GAP43. GAPDH served to monitor equal loading and transfer of samples. (B) Effects of exogenous HA-HuD and HA-R236K on inducing $p21^{cip1/waf1}$ expression. PC12 cells were transiently transfected with HA-HuD or HA-R236K, and total lysates were blotted with anti-$p21^{cip1/waf1}$, -GAP43, and -actin antibodies. The $p21^{cip1/waf1}$ protein level was significantly increased in HA-R236K-expressing cells (top panel, lane 3). The same levels of HA-tagged proteins were monitored by anti-HA blotting. (C) Upregulation of $p21^{cip1/waf1}$ mRNA in $CARM1^{-}$

asymmetric dimethylarginine antibody, which specifically recognizes asymmetrically methylated arginine residues on the Sam68 RGG repeat (18), did not detect the methylated GST-HuD (data not shown). These results suggested that the observed [^{3}H] incorporation to GST-fused HuD by CARM1 was attributable to the methylation of Arg^{236} of HuD, but we could not determine whether the detected methylarginine residue was mono- or dimethylated and, if dimethylated, whether it was symmetrically or asymmetrically methylated.

To reconfirm Arg^{236} of HuD as a methyltransferase target in PC12 cells, HA-tagged HuD harboring the Arg^{236}-to-Lys mutation (HA-R236K) was transiently expressed in the cells and immunoprecipitated with an anti-M/DMA antibody. The precipitated proteins from HA-tagged HuDwt (HA-HuDwt)-expressing cells were blotted with anti-HA antibody, while no immunoreactivity was detected with the HA-R236K-expressing cells (Fig. 1D). This result demonstrated that Arg^{236} of HuD is a major methylation site by CARM1 in PC12 cells.

To determine whether endogenous HuD is methylated by CARM1 in vivo, we established PC12 cell clones in which endogenous CARM1 expression was stably suppressed by RNA interference. Reduction of CARM1 in the stable cell lines was confirmed by immunocytochemistry (Fig. 2A) and Western blot analysis (Fig. 2B). In these clones, CARM1 expression was completely extinct, with PRMT1 and PRMT3 levels being unaffected (Fig. 2B). By use of immunocytochemistry, the dense staining in the nuclei of the parent PC12 cells was abolished in all cell lines, though faint immunoreactivities in the cytoplasm remained (Fig. 2A, panel c). The cytoplasmic CARM1 immunoreactivities are discussed below, because the observation that CARM1 resides in the cytoplasm of PC12 cells as well as in the nuclei (Fig. 2A, panels a and c) argues against previous studies demonstrating its nuclear localization (24, 70). To see whether CARM1 loss affects methylation of HuD in PC12 cells, precipitated HuD with anti-M/DMA antibody from CARM1$^-$ cells was compared with that from native PC12 cells. Though the total HuD level in the CARM1$^-$ cells was equivalent to that in the native cells (Fig. 2C, lower panel), HuD immunoreactivity precipitated with anti-M/ADMA antibody from the CARM1$^-$ cells was significantly decreased, comparable to that precipitated with the control mouse IgG (Fig. 2C, lane 3).

Subcellular localization of CARM1 in PC12 cells. In terms of subcellular localization, previous reports showed that CARM1 was localized predominantly in the nuclei of HeLa cells (24) and mouse embryonic fibroblast cells (70). In spite of no evidence for the cytoplasmic existence of CARM1, its so-far-reported substrates, PABP1 and TARPP, are both cytoplasmic proteins (2, 35), and HuD also resides in the cytoplasm of PC12 cells and induces neuronal differentiation (31, 32). A recent report demonstrated that in C2C12 myoblasts CARM1 localizes not only in the nuclei but also in the sarcoplasm (13). To consolidate the subcellular localization of CARM1 in PC12 cells, immunocytochemistry was done with HRP-diaminobenzidine tetrahydrochloride (DAB) and fluorescence-labeling methods. In HeLa cells, immunoreactivity was restricted to the nuclei by both methods, as previously reported, with almost no significant staining in the cytoplasm (Fig. 3A, left panels). In contrast, in the PC12 cells, unambiguous staining was identified in the cytoplasm as well as in the nuclei by both methods (Fig. 3A, middle panels). To confirm the specificity of the immunoreactivity, anti-CARM1 antiserum that was adsorbed with either recombinant GST-CARM1 or GST was applied to the PC12 cell preparations. DAB-stained signal with anti-CARM1 antibody was absorbed with GST-CARM1 (Fig. 3A, right panels) but not with GST (data not shown) in HeLa cells and PC12 cells, ruling out the possibility that the cytoplasmic staining was due to artifacts.

We further examined whether HuD and CARM1 colocalize in the cytoplasm of PC12 cells. As shown in Fig. 3B, HuD and CARM1 immunoreactivities overlapped in the cytoplasm, especially in the region centered around the nuclei rather than in the cell peripheries (Fig. 3B, panels a to c). When the cells were immunostained with another anti-HuD antibody, the colocalization was reproduced (Fig. 3C). When the CARM1$^-$ cells were immunostained, weak cytoplasmic immunoreactivity of CARM1, which did not overlap with that of HuD, was observed (Fig. 3B, panels d and f). Since the subcellular localization of HuD was not affected in the presence or absence of CARM1, Arg^{236} methylation of HuD does not act on its subcellular localization (Fig. 3B, compare panels b and e).

CARM1 depletion induces p21$^{cip1/waf1}$ expression by prolongation of the mRNA half-life. To elucidate the functional significance of HuD methylation, we examined the effect of unmethylated HuD on the growth and differentiation state of PC12 cells by using CARM1-depleted clones (no. 15, 16, and 33). We first analyzed the protein levels of p21$^{cip1/waf1}$, GAP43, tau, and p27, whose mRNA half-lives are regulated by HuD. The lysates from mock-transfected cells and three methylation-defective clones cultured in the growth media were blotted with each of the above antibodies. Inhibited methylation of HuD had no effect on tau and p27 expression levels (Fig. 4A).

clone 15. Northern blot analyses were performed with total RNAs extracted from the parental, CARM1$^-$, and NGF-treated parental PC12 cells. The basal p21$^{cip1/waf1}$ transcript level in CARM1$^-$ cells (middle column) was about threefold higher than that in the parental cells (left column), which was comparable to that in the native cells treated with NGF for 2 days (2d) (right column). Differences (*n*-fold) are indicated between the blots. GAP43 and tau transcripts made almost no difference between the parental and CARM1$^-$ cells or NGF-upregulated p21$^{cip1/waf1}$, GAP43, and tau transcript levels (right column). GAPDH mRNA served to monitor equal loading and transfer of samples. (D) The basal transcription level of the p21$^{cip1/waf1}$ gene was not affected by CARM1 depletion. Nuclei from parental, CARM1$^-$, and NGF-treated PC12 cells were isolated for nuclear run-on assay to monitor transcription rates for the genes indicated. The PCR product (1 μg) corresponding to each gene was blotted onto nitrocellulose filters. GAPDH was employed as a control gene (not induced by NGF), GAP43 as a positive control gene (induced by NGF), and green fluorescent protein (GFP) as a negative control. (E) p21$^{cip1/waf1}$ mRNA was stabilized in CARM1$^-$ PC12 cells to the extent of NGF-treated native PC12 cells. The time at which actinomycin D was added to the media is indicated as 0 h. Total RNA was prepared at each indicated time and analyzed by Northern blot analysis. (F) Quantification of half-life of p21$^{cip1/waf1}$ mRNA for each cell group. Densitometric values of p21$^{cip1/waf1}$ at every time point were plotted on a logarithmic scale. The half-life of p21$^{cip1/waf1}$ mRNA is formulated as the time at which the density was reduced to half that of the initial density. Data represent the means ± standard errors of the means from three independent experiments.

GAP43 expression level did not change in two clones but was significantly increased in clone no. 33 (Fig. 4A). However, $p21^{cip1/waf1}$ protein levels dramatically increased in all of the CARM1-depleted clones (Fig. 4A). To examine whether it was the unmethylated population of HuD that induced $p21^{cip1/waf1}$ expression, we biased the total population of HuD toward the unmethylated population by overexpressing methylation-resistant HuD (HA-R236K) in the native PC12 cells. The overexpression of HA-R236K considerably promoted $p21^{cip1/waf1}$ expression compared with the level achieved with HA-HuDwt (Fig. 4B, top panel). However, GAP43 protein levels were unchanged in the HA-R236K- and HA-HuDwt-expressing cells (Fig. 4B). Thus, the relative increases in the unmethylated population of HuD by two different methods induced a common effect on p21 protein expression. Therefore, we next explored how unmethylated HuD induces the rises in $p21^{cip1/waf1}$ protein.

When the transcript levels of $p21^{cip1/waf1}$, GAP43, and tau were compared between mock-transfected and $CARM1^-$ cell line no. 15, only $p21^{cip1/waf1}$ mRNA had a 3.26-fold increase in clone no. 15 cultured under the growth condition (Fig. 4C, top panel, compare left and middle lanes). Other transcripts examined were not so affected by the loss of CARM1 (Fig. 4C), while NGF administration upregulated all three of the transcripts to the same extent (Fig. 4C, compare the left and right lanes in each panel). To examine if the induction of $p21^{cip1/waf1}$ mRNA in $CARM1^-$ cells resulted from transactivation of the gene, we performed a nuclear run-on assay. The nuclear extract from $CARM1^-$ cells labeled an amount of $p21^{cip1/waf1}$ transcript comparable to (or rather less than) that from the parental cell (Fig. 4D, compare left and middle panels), which was different from the case of the NGF-treated native cells, whose nuclear extract could activate the transcription of both of the genes (Fig. 4D, right panel). This result raised the possibility that the rise in basal $p21^{cip1/waf1}$ transcript level could be due to an enhancement of the protective effect of HuD on the transcript, not to its transactivation.

Given that HuD was shown to bind to $p21^{cip1/waf1}$ mRNA and protect it from ARE-mediated decay, we next assayed the decay rate of $p21^{cip1/waf1}$ transcript under the condition where the total transcription level was halted by actinomycin D. In the parental cell line, NGF treatment markedly elongated the half-life of $p21^{cip1/waf1}$ mRNA from an apparent half-life of 2.4 h for the untreated group to that of 8.7 h for the NGF-treated group (Fig. 4E, top and bottom panels, and F). As expected, the CARM1-defective condition elongated the average half-life to 8.5 h, similarly to the NGF treatment (Fig. 4E, middle panel, and F). These observations indicated that the propagation of unmethylated HuD in $CARM1^-$ cells can protect $p21^{cip1/waf1}$ mRNA from the degradation pathway to elevate its expression.

Methylation state of HuD regulates its complex formation with $p21^{cip1/waf1}$ mRNA. We further tested whether an RNA-protein complex formation between HuD and $p21^{cip1/waf1}$ transcript would be regulated in a methylation-dependent manner. The association with PC12 cells was analyzed by PCR-based detection of the $p21^{cip1/waf1}$ mRNA in immunoprecipitated HuD. Template RNA for RT-PCR was extracted from the precipitated fractions with anti-HA antibody from either HA-HuDwt- or HA-R236K-expressing cells. The densitometric values of the amplified products of $p21^{cip1/waf1}$ were normalized to those of GAPDH. No amplified product was gained from the precipitated mRNA with control IgG1 from HA-HuD-expressing cells (Fig. 5A, lane 1). In comparison with anti-HA-precipitated mRNAs from HA-HuDwt-expressing cells, about a 5.8-fold increase in $p21^{cip1/waf1}$ amplified product was exhibited with HA-R236K-expressing cells (Fig. 5A, lanes 2 and 3). This means that methylation-resistant HuD interacted with more

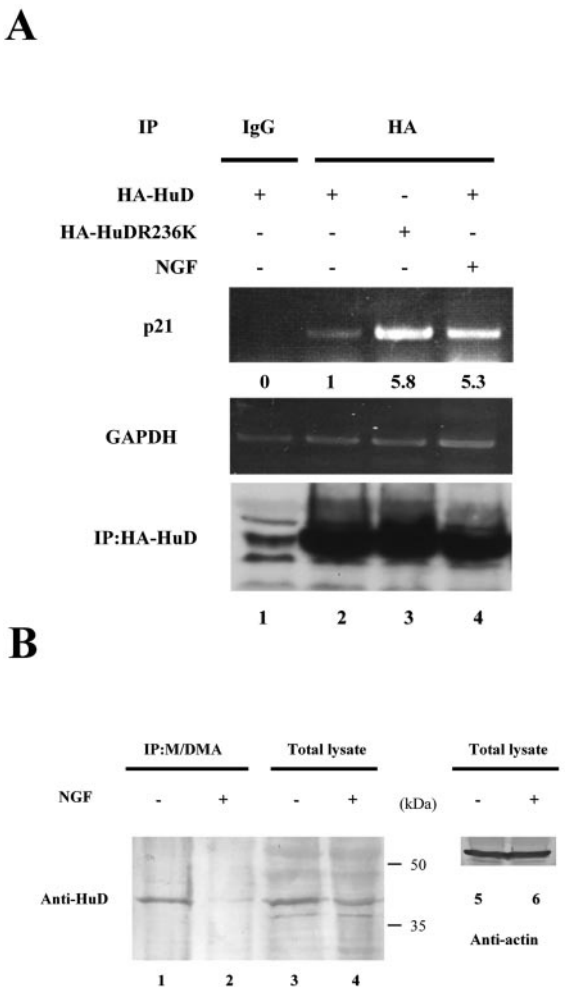

FIG. 5. Unmethylated HuD exhibited a higher binding capacity for $p21^{cip1/waf1}$ mRNA. (A) Detection by RT-PCR of p21 mRNA in materials that were precipitated with anti-HA antibody from HA-HuD- and HA-R236K-expressing cells. Control IgG1 did not yield the amplified product of $p21^{cip1/waf1}$ (top panel, lane 1) from HA-HuD-expressing cells. HA-R236K precipitated with anti-HA antibody yielded 5.8 times more PCR product of $p21^{cip1/waf1}$ than HA-HuD (top panel, lanes 2 and 3). Differences (*n*-fold) are indicated between the blots. NGF treatment propagated the amplified product of $p21^{cip1/waf1}$ from HA-HuD to the extent of HA-R236K (top panel, lane 4). Background detection of GAPDH-amplified product from each of the precipitated materials served to monitor equal use of material in each IP (middle panel). (B) NGF downregulated the methylated population of HuD. Whole-cell extracts from the untreated PC12 cells and the cells treated with NGF for 3 days were loaded directly (lanes 3 and 4) or subjected to IP with anti-M/DMA antibody (lanes 1 and 2), and they were blotted with anti-HuD antibody. Antiactin antibody blotting of the total lysates confirmed the same protein load (lanes 5 and 6).

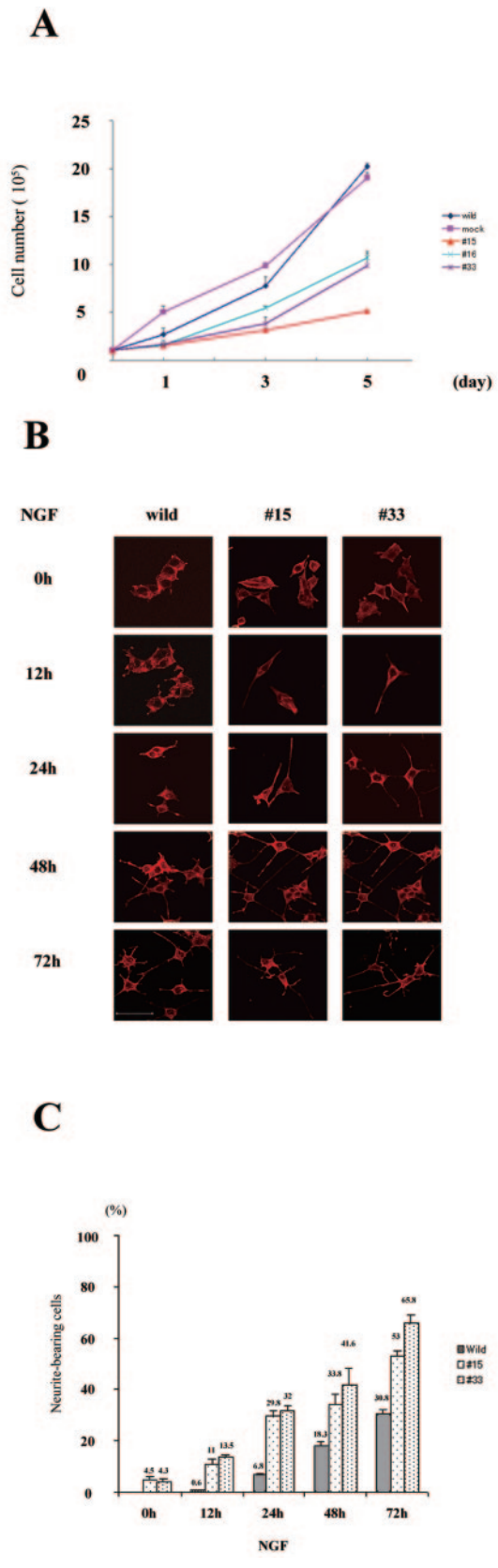

FIG. 6. Effects of CARM1 loss on proliferation and NGF-induced neurite outgrowth. (A) Comparison of levels of proliferation in parent, mock-transfected, and CARM1-depleted cells. PC12 cells were plated on 6-well dishes at a density of 1×10^5 cells per well. The cells were then cultured in growth medium and counted by a hematocytometer at every 24-h interval. Cell numbers represent the mean values from triplicate experiments. CARM1-defective cells (no. 15, 16, and 33) showed slower growth rates than parental and mock-transfected cells. (B) CARM1 depletion promoted a susceptibility to NGF-induced neurite outgrowth. Parental PC12 cells and CARM1$^-$ cells were plated on collagen-coated, 4-well-chamber slides at a density of 1×10^4 cells per well. Microscopic images of the parent and CARM1$^-$ PC12 cells (no. 15 and 33) are shown. Cultures were fixed at the indicated times after the onset of NGF exposure and stained with tetramethyl rhodamine isothiocyanate-labeled phalloidin (red). (C) Quantification of the results shown in panel B. The cells that had at least one neurite with a length covering two cell bodies in diameter was counted as neurite bearing. The error bars represent standard deviations from triplicate results. Approximately 200 cells were counted for each sample.

p21$^{cip1/waf1}$ mRNA than did the wild type. Interestingly, when HA-HuD-expressing cells were treated with NGF, p21$^{cip1/waf1}$ was amplified from the HA-precipitated mRNA to a level comparable to that for HA-R236K-expressing cells (Fig. 5A, lane 4). Then we investigated how the in vivo methylation state of endogenous HuD alters during the course of NGF-induced differentiation of PC12 cells. At 3 days after NGF treatment, HuD protein precipitated with anti-M/DMA antibody was extinguished, with the total HuD level almost unchanged (Fig. 5B). These data indicated that NGF may reduce the Arg^{236} methylation level of HuD during neuronal differentiation to enhance the direct or indirect interaction of HuD with p21$^{cip1/waf1}$ mRNA.

Inhibited methylation of HuD decreases growth rate and facilitates neurite outgrowth following NGF treatment. To characterize the phenotype of CARM1$^-$ cells, we compared these cells with the wild-type and mock-transfected cells in growth and neuritogenic activity. When we first examined the growth rates of CARM1$^-$ clones, they all exhibited much slower proliferative rates than did wild-type and mock-transfected clones ($P < 0.01$) (Fig. 6A). In addition, CARM1$^-$ clones had a tendency to extend their neurites in response to NGF. Some of the CARM1$^-$ clones extended neurites with lengths more than twice the diameter of their cell body, even in the growth media (Fig. 6B and C). In the case of the parental PC12 clone, less than 10% of the cells displayed prominent neurite outgrowth 12 to 24 h after NGF treatment (Fig. 6B). By contrast, about 12 and 31% of CARM1$^-$ cells developed neurites at 12 h and 24 h after NGF administration, respectively (Fig. 6B and C). The optimal neurite lengths of CARM1$^-$ clones at 48 h after NGF administration were larger than those of parental cells at 72 h, which amounted to the average lengths of CARM1$^-$ clones at 24 h. Together with the fact that p21$^{cip1/waf1}$ can inhibit proliferation and accelerate neurite outgrowth in response to NGF (72), it is possible that the lowered level of methylated HuD in the CARM1$^-$ cells can promote p21$^{cip1/waf1}$ expression by the protective effect of unmethylated HuD on its transcripts to make a differentiated phenotype for the cells.

CARM1 in the adult mouse brain partially colocalizes with BrdU-positive cells. The above-described data raised the possibility that CARM1 maintains the cells in the proliferative state. To investigate the correlation between CARM1 and cell proliferation, BrdU-labeled adult mouse brain was doubly stained with anti-CARM1 and anti-BrdU antibodies. While BrdU-positive cells were densely distributed along the ventric-

FIG. 7. Distribution of CARM1-expressing cells in the adult mouse brain. Immunofluorescent double staining of the VZ was achieved by use of the antibodies to CARM1 (green) (a) and BrdU (red) (b). In the adult mouse brain, CARM1-expressing cells were mainly observed in the lateral VZ and dentate gyrus. Some CARM1-expressing cells in the lateral ventricular wall are costained with BrdU (c). LV, lateral ventricle.

ular zone (VZ) (Fig. 7b), CARM1 distribution ranged from the VZ to the ventricular border of the subventricular zone (Fig. 7a), in which the arrested cells start radial migration from the VZ. More than 60% of BrdU-positive cells displayed CARM1 immunoreactivity (Fig. 7c) in the VZ, suggesting that most of the CARM1-expressing cells have the competence to proliferate. Thus, CARM1 was involved in the proliferation of neural cell precursors.

DISCUSSION

Aletta's group reported that protein methyltransferase inhibitors completely blocked NGF-induced neurite extension of PC12 cells without affecting their viability and proliferative activity and that the required methyltransferase activity for neurite extension might be due chiefly to asymmetric arginine dimethylation and not to methylation of nucleotides or other amino acid residues (16, 17). Among the substrates for arginine methyltransferases, we noted RBPs, some of which proved to be involved in neuronal differentiation. Fortunately, one of the RBPs, HuR, was shown to be methylated in vitro and in vivo by CARM1 arginine methyltransferase (41). HuR belongs to the Hu/ELAV RBP family and regulates ARE-mediated mRNA decay by competing with AUF decay-promoting factors for ARE-containing mRNA (38, 63). The alignment of the amino acid sequence around the dimethylated arginine residue of HuR displays a high sequence homology with that of the other mammalian Hu members (28, 52). Then we focused on a neuron-specific Hu family protein, HuD, as the methylated substrate and examined whether or how its methylation regulates the turnover of the bound mRNAs in PC12 cells.

Using an in vitro protein methylation assay, we showed that HuD is a specific substrate for CARM1. ^{3}H-labeled HuD was blotted with an antibody against mono- and dimethylarginine, which was used to demonstrate in vivo methylation of HuR (41). The anti-M/DMA antibody immunoprecipitated endogenous HuD from the lysate of native PC12 cells but not that of CARM1^{-} cell lines that we established (Fig. 2C). It also precipitated exogenous HuD from HuDwt-transfected PC12 cell lysate but not that from R236K-transfected cells (Fig. 1D). These data demonstrate that Arg^{236} is a major CARM1 methylation site, both in vitro and in vivo, which corresponds to Arg^{217} of HuR. Since the antibody towards methylarginine residues used in this study was incapable of sufficiently identifying the style of arginine methylation, we had to determine it by mass spectrometry.

Our data argued against the previous reports on CARM1 subcellular localization. In HeLa cells and primary fibroblasts, CARM1 was shown to reside predominantly in the nucleus (24, 70). If this were the case with PC12 cells, CARM1 would be sequestered from HuD by the nuclear membrane. However, our DAB-stained preparation and fluorescence immunocytochemistry analysis revealed substantial CARM1 reactivity in the cytoplasm of PC12 cells (Fig. 3A). CARM1 cytoplasmic staining was somewhat obscure compared to the intense nuclear immunoreactivity and was left at the level reminiscent of the background staining in CARM1^{-} cells, which completely lost the nuclear staining. To exclude the possibility that the cytoplasmic staining is an artifact, antiserum adsorbed with GST-CARM1 was used for CARM1 immunodetection by the DAB staining method. Because the adsorbed antiserum failed to react with any epitopes in the cytoplasm or in the nucleus (Fig. 3A), the observed cytoplasmic staining with PC12 cells reflected CARM1 immunoreactivity. A recent study demonstrated cytoplasmic localization of CARM1 in C2C12 myoblasts (13), indicating that CARM1 localization is cell type dependent. We further demonstrated a colocalization of CARM1 and HuD in the cytoplasm, which surrounded the nucleus and was extinguished around the cell periphery. We further investigated whether methylation affects the subcellular localization, because Arg^{236} is located in the hinge region that determines the subcellular localization (32). As shown in Fig. 3B, the Arg^{236} methylation level had no effect on the subcellular localization of HuD.

We next examined the effects of HuD methylation on innate function, such as nucleic acid-binding property. Since GAR domains are methylated in a variety of RBPs (18, 25, 26, 37, 49), their methylation possibly influences the protein-RNA interactions. For example, the unmethylated form of hnRNP A1 has a higher binding capacity to single-stranded nucleic acids than the methylated form (55). Arginine methylation of HuD may also modulate its direct interaction with ARE-containing mRNAs; otherwise, the methylation event may regulate an interaction with another protein which controls the RNA-binding interface of HuD, RRM2 and/or RRM3 (53). We then investigated expression levels of the genes whose transcripts are regulated by HuD in CARM1^{-} PC12 cells. Although CARM1 knockdown had no effect on the protein and transcript levels of GAP43, tau, and p27, it exclusively upregulated those of $p21^{cip1/waf1}$ (Fig. 4A and C). We confirmed that the rise in $p21^{cip1/waf1}$ transcripts was due not to the enhancement of its transcription (Fig. 4D) but to the elongation of its half-life (Fig. 4E and F). We further demonstrated that the methylation-resistant HuD mutant R236K made a complex with $p21^{cip1/waf1}$ mRNA to a greater extent than did methylated HuD (Fig. 5A). These results indicated that unmethylated HuD could lower the decay rate of $p21^{cip1/waf1}$ transcript by forming a tighter complex with it. HuD was reported to act on a variety of ARE-containing mRNAs, but the only gene product affected by CARM1 loss was $p21^{cip1/waf1}$, according to our examination. Though ARE-containing GAP43 mRNA is stabilized by HuD modifying its poly(A) tail length (10) and is associated with HuD in the growth cones of PC12 cells (59), CARM1 depletion had no effect on GAP43

transcript level and decay rate (Fig. 4A, C, and E). We inferred that RNP complex components other than HuD might be different among $p21^{cip1/waf1}$ and GAP43 transcripts and that those of $p21^{cip1/waf1}$ are influenced primarily by methylation of HuD. Since the methylation state of HuD could possibly affect the turnover of unknown transcripts, we attempted to make a catalogue of transcripts with differential binding characters to methylated and unmethylated HuD by use of a microarray-based method.

To investigate whether HuD is the sole mediator for producing such gene expression patterns in $CARM1^-$ cells, we introduced an excess amount of the methylation-resistant HuD mutant R236K into native PC12 cells (Fig. 4B). The overexpression of naked HuD remarkably induced $p21^{cip1/waf1}$ protein without affecting the GAP43 protein level, demonstrating that a higher ratio of unmethylated HuD only by overexpression of methylation-defective HuD could reproduce the CARM1-defective phenotype. Though there remained the possibility that other CARM1 substrates, especially other neuron-specific Hu family proteins HuB and HuC, are relevant to the induction of $p21^{cip1/waf1}$ transcripts, our data strongly suggested that the unmethylated protein HuD is sufficient to cause the same effect as CARM1 depletion. Even though HuB and HuC are similarly regulated by CARM1, there is no direct evidence of their interaction with $p21^{cip1/waf1}$ transcripts.

Interestingly, methylated HuD was extinct 3 days after NGF treatment with PC12 cells, even when total HuD was kept at the steady-state level (Fig. 5B). This observation indicated that NGF could produce the same effect on HuD as CARM1 depletion, in keeping with our result that NGF induced $p21^{cip1/waf1}$ transcript to an extent similar to that induced by CARM1 depletion (Fig. 4B). Note that $CARM1^-$ cells exhibited a slow growth rate (Fig. 6A) and accelerated neurite extension (Fig. 6B and C), which also occurs in the NGF-treated PC12 cells; thus, it is possible that the loss of methylated HuD and the resultant rise in $p21^{cip1/waf1}$ mRNA may be one of the major processes for the NGF signaling pathway. To explain how NGF decreases the methylated population of HuD with the total amount being unchanged, we assume that, once methylated, HuD is enzymatically demethylated at the onset of NGF signaling. Recently, monomethyl-arginine residues on H3 and H4 histone proteins were shown to be methyl-deiminated to citrulline by protein arginine deiminase 4 (PAD4) (19, 68). However, since this kind of reaction has been shown to act on monomethylated arginine, a novel system might be required for elimination or oxidization of the methyl group from arginine-methylated HuD.

Altogether, the methylated state of HuD determines the $p21^{cip1/waf1}$ expression level, and the inhibited methyltransferase activity of CARM1 can arrest the growth of PC12 cells to represent a partially differentiated cell shape by propagating unmethylated HuD. Accordingly, our results are inconsistent with previous reports that protein arginine methylation is required for NGF-induced differentiation of PC12 cells (16). In fact, these reports evaluated the whole effect of protein methylation by using methyltransferase inhibitors with broad spectra, whereas we focused on the effect of selective inhibition of CARM1. Compared with PRMT1, CARM1 activity covers a limited species of proteins (39). This is why our results are discrepant with the general inhibition of arginine methylation that abrogated NGF-induced neuritogenesis of PC12.

In conclusion, our data demonstrated that CARM1 methylates Arg^{236} of HuD in vitro and in vivo and that the methylation of HuD raised the vulnerability of $p21^{cip1/waf1}$ transcripts to direct PC12 cells to the proliferative state, whereas unmethylated HuD endowed the cells with differentiated phenotypes in an NGF-independent manner. Our final observation, that CARM1-expressing cells were localized in the VZ of the lateral ventricle of the adult mouse brain and overlapped with BrdU-positive cells (Fig. 7), supports the notion that CARM1 keeps the cells in the proliferative state.

REFERENCES

1. **Abe, R., E. Sakashita, K. Yamamoto, and H. Sakamoto.** 1996. Two different RNA binding activities for the AU-rich element and the poly(A) sequence of the mouse neuronal protein mHuC. Nucleic Acids Res. **24:**4895–4901.
2. **Afonina, E., R. Stauber, and G. N. Pavlakis.** 1998. The human poly(A)-binding protein 1 shuttles between the nucleus and the cytoplasm. J. Biol. Chem. **273:**13015–13021.
3. **Akamatsu, W., H. Fujihara, T. Mitsuhashi, M. Yano, S. Shibata, Y. Hayakawa, H. J. Okano, S. Sakakibara, H. Takano, T. Takano, T. Takahashi, T. Noda, and H. Okano.** 2005. The RNA-binding protein HuD regulates neuronal cell identity and maturation. Proc. Natl. Acad. Sci. USA **102:**4625–4630.
4. **An, W., J. Kim, and R. G. Roeder.** 2004. Ordered cooperative functions of PRMT1, p300, and CARM1 in transcriptional activation by p53. Cell **117:**735–748.
5. **Anderson, K. D., J. Sengupta, M. Morin, R. L. Neve, C. F. Valenzuela, and N. I. Perrone-Bizzozero.** 2001. Overexpression of HuD accelerates neurite outgrowth and increases GAP-43 mRNA expression in cortical neurons and retinoic acid-induced embryonic stem cells in vitro. Exp. Neurol. **168:**250–258.
6. **Antic, D., and J. D. Keene.** 1997. Embryonic lethal abnormal visual RNA-binding proteins involved in growth, differentiation, and posttranscriptional gene expression. Am. J. Hum. Genet. **61:**273–278.
7. **Antic, D., N. Lu, and J. D. Keene.** 1999. ELAV tumor antigen, Hel-N1, increases translation of neurofilament M mRNA and induces formation of neurites in human teratocarcinoma cells. Genes Dev. **13:**449–461.
8. **Aoki, K., Y. Ishii, K. Matsumoto, and M. Tsujimoto.** 2002. Methylation of *Xenopus* CIRP2 regulates its arginine- and glycine-rich region-mediated nucleocytoplasmic distribution. Nucleic Acids Res. **30:**5182–5192.
9. **Aranda-Abreu, G. E., L. Behar, S. Chung, H. M. Furneaux, and I. Ginzburg.** 1999. Embryonic lethal abnormal vision-like RNA-binding proteins regulate neurite outgrowth and tau expression in PC12 cells. J. Neurosci. **19:**6907–6917.
10. **Beckel-Mitchener, A. C., A. Miera, R. Keller, and N. I. Perrone-Bizzozero.** 2002. Poly(A) tail length-dependent stabilization of GAP-43 mRNA by the RNA-binding protein HuD. J. Biol. Chem. **277:**27996–28002.
11. **Burd, C. G., and G. Dreyfuss.** 1994. Conserved structures and diversity of functions of RNA-binding proteins. Science **265:**615–621.
12. **Chen, D., H. Ma, H. Hong, S. S. Koh, S. M. Huang, B. T. Schurter, D. W. Aswad, and M. R. Stallcup.** 1999. Regulation of transcription by a protein methyltransferase. Science **284:**2174–2177.
13. **Chen, S. L., K. A. Loffler, D. Chen, M. R. Stallcup, and E. O. Muscat.** 2002. The coactivator-associated arginine methyltransferase is necessary for muscle differentiation: CARM1 coactivates myocyte enhancer factor-2. J. Biol. Chem. **277:**4324–4333.
14. **Chung, S. M., L. Jiang, S. Cheng, and H. M. Furneaux.** 1996. Purification and properties of HuD, a neuronal RNA-binding protein. J. Biol. Chem. **271:**11518–11524.
15. **Chung, S. M., M. Eckrich, N. I. Perrone-Bizzozero, D. T. Kohn, and H. M. Furneaux.** 1997. The Elav-like proteins bind to a conserved regulatory element in the 3′-untranslated region of GAP-43 mRNA. J. Biol. Chem. **272:**6593–6598.
16. **Cimato, T. R., M. J. Ettinger, X. Zhou, and J. M. Aletta.** 1997. Nerve growth factor-specific regulation of protein methylation during neuronal differentiation of PC12 cells. J. Cell Biol. **138:**1089–1103.
17. **Cimato, T. R., J. Tang, Y. Xu, C. Guarnaccia, H. R. Herschman, S. Pongor, and J. M. Aletta.** 2002. Nerve growth factor-mediated increases in protein methylation occur predominantly at type I arginine methylation sites and involve protein arginine methyltransferase 1. J. Neurosci. Res. **67:**435–442.
18. **Côté, J., F.-M. Boisvert, M.-C. Boulanger, M. T. Bedford, and S. Richard.** 2003. Sam68 RNA binding protein is an in vivo substrate for protein arginine *N*-methyltransferase 1. Mol. Biol. Cell **14:**274–287.
19. **Cuthbert, G. L., S. Daujat, A. W. Snowden, H. Erdjument-Bromage, T. Hagiwara, M. Yamada, R. Schneider, P. D. Gregory, P. Tempst, A. J. Bannister,**

and T. Kouzarides. 2004. Histone deimination antagonizes arginine methylation. Cell **118:**545–553.
20. **Dalmau, J., H. M. Furneaux, C. Cordon-Cardo, and J. B. Posner.** 1992. The expression of the Hu (paraneoplastic encephalomyelitis/sensory neuronopathy) antigen in human normal and tumor tissues. Am. J. Pathol. **141:**881–886.
21. **Deschênes-Furry, J., G. Bélanger, N. Perrone-Bizzozero, and B. J. Jasmin.** 2003. Post-transcriptional regulation of acetylcholinesterase mRNAs in nerve growth factor-treated PC12 cells by the RNA-binding protein HuD. J. Biol. Chem. **278:**5710–5717.
22. **Erhardt, J. A., and R. N. Pittmann.** 1998. p21WAF1 induces permanent growth arrest and enhances differentiation, but does not alter apoptosis in PC12 cells. Oncogene **16:**443–451.
23. **Fan, X. C., and J. A. Steitz.** 1998. Overexpression of HuR, a nuclear-cytoplasmic shuttling protein, increases the *in vivo* stability of ARE-containing mRNAs. EMBO J. **17:**3448–3460.
24. **Frankel, A., N. Yadav, J. Lee, T. L. Branscombe, S. Clarke, and M. T. Bedford.** 2002. The novel human protein arginine *N*-methyltransferase PRMT6 is a nuclear enzyme displaying unique substrate specificity. J. Biol. Chem. **277:**3537–3543.
25. **Frankel, A., and S. Clarke.** 2000. PRMT3 is a distinct member of the protein arginine *N*-methyltransferase family. J. Biol. Chem. **275:**32974–32982.
26. **Gary, J. D., and S. Clarke.** 1998. RNA and protein interactions modulated by protein arginine methylation. Prog. Nucleic Acid Res. Mol. Biol. **61:**65–131.
27. **Good, P. J.** 1995. A conserved family of *elav*-like genes in vertebrates. Proc. Natl. Acad. Sci. USA **92:**4557–4561.
28. **Good, P. J.** 1997. The role of *elav*-like genes, a conserved family encoding RNA-binding proteins, in growth and development. Semin. Cell Dev. Biol. **8:**577–584.
29. **Jain, R. G., L. G. Andrews, K. M. McGowan, P. H. Pekala, and J. D. Keene.** 1997. Ectopic expression of Hel-N1, an RNA-binding protein, increases glucose transporter (GLUT1) expression in 3T3-L1 adipocytes. Mol. Cell. Biol. **17:**954–962.
30. **Joseph, B., M. Orlian, and H. Furneaux.** 1998. $p21^{waf1}$ mRNA contains a conserved element in its 3′-untranslated region that is bound by the Elav-like mRNA-stabilizing proteins. J. Biol. Chem. **273:**20511–20516.
31. **Kasashima, K., E. Sakashita, K. Saito, and H. Sakamoto.** 2002. Complex formation of the neuron-specific ELAV-like Hu RNA-binding proteins. Nucleic Acids Res. **30:**4519–4526.
32. **Kasashima, K., K. Terashima, K. Yamamoto, E. Sakashita, and H. Sakamoto.** 1999. Cytoplasmic localization is required for the mammalian ELAV-like protein HuD to induce neuronal differentiation. Genes Cells **4:**667–683.
33. **Keene, J. D.** 1999. Why is Hu where? Shuttling of early-response-gene messenger RNA subsets. Proc. Natl. Acad. Sci. USA **96:**5–7.
34. **Kim, S., B. M. Merrill, R. Rajpurohit, A. Kumar, K. L. Stone, V. V. Papov, J. M. Schneiders, W. Szer, S. H. Wilson, W. K. Paik, and K. R. Williams.** 1997. Identification of N^G-methylarginine residues in human heterogeneous RNP protein A1: Phe/Gly-Gly-Gly-Arg-Gly-Gly-Gly/Phe is a preferred recognition motif. Biochemistry **36:**5185–5192.
35. **Kisielow, J., A. C. Nairn, and K. Karjalainen.** 2001. TARPP, a novel protein that accompanies TCR gene rearrangement and thymocyte education. Eur. J. Immunol. **31:**1141–1149.
36. **Kullmann, M., U. Gopfert, B. Siewe, and L. Hengst.** 2002. ELAV/Hu proteins inhibit p27 translation via an IRES element in the p27 5′ UTR. Genes Dev. **16:**3087–3099.
37. **Kzhyshkowska, J., H. Schutt, M. Liss, E. Kremmer, R. Stauber, H. Wolf, and T. Dobner.** 2001. Heterogeneous nuclear ribonucleoprotein E1B-AP5 is methylated in its Arg-Gly-Gly (RGG) box and interacts with human arginine methyltransferase HRMT1L1. Biochem. J. **358:**305–314.
38. **Lal, A., K. Mazan-Mamczarz, T. Kawai, X. Yang, J. L. Martindale, and M. Gorospe.** 2004. Concurrent versus individual binding of HuR and AUF1 to common labile target mRNAs. EMBO J. **23:**3092–3102.
39. **Lee, J., and M. T. Bedford.** 2002. PABP1 identified as an arginine methyltransferase substrate using high-density protein arrays. EMBO Rep. **3:**268–273.
40. **Levine, T. D., F. Gao, P. H. King, L. G. Andrews, and J. D. Keene.** 1993. Hel-N1: an autoimmune RNA-binding protein with specificity for 3′ uridylate-rich untranslated regions of growth factor mRNAs. Mol. Cell. Biol. **13:**3494–3504.
41. **Li, H., S. Park, B. Kilburn, M. A. Jelinek, A. Henschen-Edman, D. W. Aswad, M. R. Stallcup, and I. A. Laird-Offringa.** 2002. Lipopolysaccharide-induced methylation of HuR, an mRNA-stabilizing protein, by CARM1. J. Biol. Chem. **277:**44623–44630.
42. **Liu, J., J. Dalmau, A. Szabo, M. Rosenfeld, J. Huber, and H. M. Furneaux.** 1995. Paraneoplastic encephalomyelitis antigens bind to the AU-rich elements of mRNA. Neurology **45:**544–550.
43. **Liu, Q., and G. Dreyfuss.** 1995. In vivo and in vitro arginine methylation of RNA-binding proteins. Mol. Cell. Biol. **15:**2800–2808.
44. **Ma, H., C. Baumann, H. Li, B. Strahl, R. Rice, M. Jelinek, D. Aswad, C. Allis, G. Hager, and M. Stallcup.** 2001. Hormone-dependent, CARM1-directed, arginine-specific methylation of histone H3 on a steroid-regulated promoter. Curr. Biol. **11:**1981–1985.
45. **Ma, W. J., S. Cheng, C. Campbell, A. Wright, and H. M. Furneaux.** 1996. Cloning and characterization of HuR, a ubiquitously expressed Elav-like protein. J. Biol. Chem. **271:**8144–8151.
46. **Ma, W. J., S. Chung, and H. M. Furneaux.** 1997. The Elav-like proteins bind to AU-rich elements and to the poly(A) tail of mRNA. Nucleic Acids Res. **25:**3564–3569.
47. **Mears, W. E., and S. A. Rice.** 1996. The RGG box motif of the herpes simplex virus ICP27 protein mediates an RNA-binding activity and determines in vivo methylation. J. Virol. **70:**7445–7453.
48. **Mobarak, C. D., K. D. Andrson, M. Morin, A. Beckel-Mitchener, S. L. Rogers, H. M. Furneaux, P. King, and N. I. Perrone-Bizzozero.** 2000. The RNA-binding protein HuD is required for GAP-43 mRNA stability, GAP-43 gene expression, and PKC-dependent neurite outgrowth in PC12 cells. Mol. Biol. Cell **11:**3191–3203.
49. **Najbauer, J., B. A. Johnson, A. L. Young, and D. W. Aswad.** 1993. Peptides with sequences similar to glycine, arginine-rich motifs in proteins interacting with RNA are efficiently recognized by methyltransferase(s) modifying arginine in numerous proteins. J. Biol. Chem. **268:**10501–10509.
50. **Nichols, R. C., X. W. Wang, J. Tang, B. J. Hamilton, F. A. High, H. R. Herschman, and W. F. C. Rigby.** 2000. The RGG domain in hnRNP A2 affects subcellular localization. Exp. Cell Res. **256:**522–532.
51. **Ohkura, N., M. Takahashi, H. Yaguchi, Y. Nagamura, and T. Tsukada.** 2005. Coactivator-associated arginine methyltransferase 1, CARM1, affects pre-mRNA splicing in an isoform-specific manner. J. Biol. Chem. **280:**28927–28935.
52. **Okano, H. J., and R. B. Darnell.** 1997. A hierarchy of Hu RNA binding proteins in developing and adult neurons. J. Neurosci. **17:**3024–3037.
53. **Park, S., D. G. Myszka, M. Yu, S. J. Littler, and I. A. Laird-Offringa.** 2000. HuD RNA recognition motifs play distinct roles in the formation of a stable complex with AU-rich RNA. Mol. Cell. Biol. **20:**4765–4772. (Erratum, **24:** 6888, 2004.)
54. **Park-Lee, S., S. Kim, and I. A. Laird-Offringa.** 2003. Characterization of the interaction between neuronal RNA-binding protein HuD and AU-rich RNA. J. Biol. Chem. **278:**39801–39808.
55. **Rajpurohit, R., W. K. Paik, and S. Kim.** 1994. Effect of enzymic methylation of heterogeneous ribonucleoprotein particle A1 on its nucleic-acid binding and controlled proteolysis. Biochem. J. **304:**903–909.
56. **Robinow, S., A. R. Campos, K. M. Yao, and K. White.** 1988. The elav gene product of Drosophila, required in neurons, has three RNP consensus motifs. Science **242:**1570–1572. (Erratum, **243:**12, 1989.)
57. **Siebel, C. W., and C. Guthrie.** 1996. The essential yeast RNA binding protein Np13p is methylated. Proc. Natl. Acad. Sci. USA **93:**13641–13646.
58. **Siomi, H., and G. Dreyfuss.** 1997. RNA-binding proteins as regulators of gene expression. Curr. Opin. Genet. Dev. **7:**345–353.
59. **Smith, C. L., R. Afroz, G. J. Bassell, H. M. Furneaux, N. I. Perrone-Bizzozero, and R. W. Burry.** 2004. GAP-43 mRNA in growth cones is associated with HuD and ribosomes. J. Neurobiol. **61:**222–235.
60. **Smith, J. J., K. P. Rucknagel, A. Schierhorn, J. Tang, A. Nemeth, M. Linder, H. R. Herschman, and E. Wahle.** 1999. Unusual sites of arginine methylation in poly(A)-binding protein II and in vitro methylation by protein arginine methyltransferases PRMT1 and PRMT3. J. Biol. Chem. **274:** 13229–13234.
61. **Smith, W. A., B. T. Schurter, F. Wong-Staal, and M. David.** 2004. Arginine methylation of RNA helicase A determines its subcellular localization. J. Biol. Chem. **279:**22795–22798.
62. **Strahl, B. D., S. D. Briggs, C. J. Brame, J. A. Caldwell, S. S. Koh, H. Ma, R. G. Cook, J. Shabanowitz, D. F. Hunt, M. R. Stallcup, and C. D. Allis.** 2001. Methylation of histone H4 at arginine 3 occurs in vivo and is mediated by the nuclear receptor coactivator PRMT1. Curr. Biol. **11:**996–1000.
63. **Sully, G., J. L. E. Dean, R. Wait, L. Rawlinson, T. Santalucia, J. Saklatvala, and A. R. Clark.** 2004. Structural and functional dissection of a conserved destabilizing element of cyclo-oxygenase-2 mRNA: evidence against the involvement of AUF-1 [AU-rich element/poly(U)-binding/degradation factor-1], AUF-2, tristetraprolin, HuR (Hu antigen R) or FBP1 (far-upstream-sequence-element-binding protein 1). Biochem. J. **377:**629–639.
64. **Szabo, A., J. Dalmau, G. Manley, M. Rosenfeld, E. Wong, J. Henson, J. B. Posner, and H. M. Furneaux.** 1991. HuD, a paraneoplastic encephalomyelitis antigen, contains RNA-binding domains and is homologous to Elav and Sex-lethal. Cell **67:**325–333.
65. **Tang, J., A. Frankel, R. J. Cook, S. Kim, W. K. Paik, K. R. Williams, S. Clarke, and H. R. Herschman.** 2000. PRMT1 is the predominant type I protein arginine methyltransferase in mammalian cells. J. Biol. Chem. **275:** 7723–7730.
66. **Tang, J., J. D. Gary, S. Clarke, and H. R. Herschman.** 1998. PRMT3, a type I protein arginine *N*-methyltransferase that differs from PRMT1 in its oligomerization, subcellular localization, substrate specificity, and regulation. J. Biol. Chem. **273:**16935–16945.

67. **Valentini, S. R., V. H. Weiss, and P. A. Silver.** 1999. Arginine methylation and binding of Hrp1p to the efficiency element for mRNA 3′-end formation. RNA **5:**272–280.
68. **Wang, Y., J. Wysocka, J. Sayegh, Y.-H. Lee, J. R. Perlin, L. Leonelli, L. S. Sonbuchner, C. H. McDonald, R. G. Cook, Y. Dou, R. G. Roeder, S. Clarke, M. R. Stallcup, C. D. Allis, and S. A. Coonrod.** 2004. Human PAD4 regulates histone arginine methylation levels via demethylimination. Science **306:**279–283.
69. **Xu, W., H. Chen, K. Du, H. Asahara, M. Tini, B. M. Emerson, M. Montminy, and R. M. Evans.** 2001. A transcriptional switch mediated by cofactor methylation. Science **294:**2507–2511.
70. **Yadav, N., J. Lee, J. Kim, J. Shen, M. C.-T. Hu, C. M. Aldaz, and M. T. Bedford.** 2003. Specific protein methylation defects and gene expression perturbations in coactivator-associated arginine methyltransferase 1-deficient mice. Proc. Natl. Acad. Sci. USA **100:**6464–6468.
71. **Yan, G.-Z., and E. B. Ziff.** 1995. NGF regulates the PC12 cell cycle machinery through specific inhibition of the Cdk kinases and induction of cyclin D1. J. Neurosci. **15:**6200–6212.
72. **Yan, G.-Z., and E. B. Ziff.** 1997. Nerve growth factor induces transcription of the p21 WAF1/CIP1 and cyclin D1 genes in PC12 cells by activating the Sp1 transcription factor. J. Neurosci. **17:**6122–6132.